

Epoch Time Assisted Orbit Determination for Near Equatorial Low Earth Orbiting Satellites

Hilmi Sanusi
 Electronic System Lab (ESL)
 Dept. of Electrical and Electronic Engineering
 University of Stellenbosch, Stellenbosch 7600
 South Africa
 Email: hilmi@ing.sun.ac.za Tel: 27 21 808 4472

Jan J. du Plessis
 Dept. of Electrical and Electronic Engineering
 University of Stellenbosch, Stellenbosch 7600
 South Africa
 Email: jjdp@ing.sun.ac.za Tel: 27 21 808 4023

Abstract:

GPS (Global Position Systems) have been widely used on microsatellites to provide the ephemerid but availability of the GPS measurement cannot be guaranteed. Orbit estimators based on celestial objects from available attitude sensors with a fraction of additional computing power are attractive alternatives but lacks of accuracy. On the other hand, an orbit propagator with frequent measurement updates can provide the needed accuracy. Solving the ephemerid at the entrance and exit point of eclipse, which is used to readjust the orbit propagator is suggested in this paper. The Keplerian elements are split into slow varying elements $[a, e, i]$ and fast varying elements $[\mathbf{w}, \mathbf{W}, \mathbf{u}]$ where the slow varying elements are constantly being estimated using a Kalman filter from magnetometer data. The true anomaly, \mathbf{u} is then solved from the epoch time measured at the entrance or exit point of the eclipse later used to solve the other elements. This is possible because the uniqueness of the equatorial orbit configuration at eclipse for a given sun vector, will result in a unique solution set where the most probable answer can be selected. Having the ephemerid at eclipse point, the subsequent orbit elements in between the eclipse points can be obtained using orbit propagator while frequent updates to this orbit propagator will maintain its accuracy within its limit.

Introduction

Positioning a satellite in near equatorial orbit will benefit the countries in the equatorial region as it will pass more frequent. For continuous coverage in this region, the number of satellites needed for the constellation in this arrangement is therefore minimise.

With the current trend, most of the micro-satellites are now equipped with a sun sensor, magnetometer and horizon sensor to acquire attitude information, at the same time the same sensor also can be used to determine the orbit autonomously. This can be used as a backup to provide the orbit information when necessary.

Unfortunately, because of the constraint in weight, space and budget for most of the micro satellites, some of the sensors are not functioning optimally. As an example, the earth magnetic field only varies between ± 35 microTesla in near equatorial region (for an altitude of 800km) making accurate magnetic measurement difficult. To worsen the problem, the

earth magnetic model based on International Geomagnetic Reference Model (IGRF) is badly modelled in this region. According to recent information from the Ørsted satellite, the earth magnetic field direction is skewed due to solar wind during high sun activity. One might suggest a better resolution magnetometer, but such magnetometers are not only more expensive, but also require better reference model to be used as a filter's innovator. A higher order geomagnetic model is needed for more precise reference model, which require rigorous computation.

Reference [1]-[9] used the earth magnetic field as a navigation tool, but based on the problem mention above, this is not a good option. Reference [10]-[11], used scanning horizon sensor for this purpose, but it is not only expensive but the weight also makes it not practical for a micro satellite. Horizon sensor based on a CCD, need attitude information to be used for this principle.

Good orbit information will definitely give better attitude information. A good environment model will also give better attitude information. The aim of the study is to

refine the orbit information based on the established method [1]-[9] and to adapt it to be used in equatorial region. The final challenge of the study is to determine IGRF correction terms so that the model can be corrected continuously which in turn will give better attitude information.⁵ This definitely will help the placement of near equatorial region satellites without modifying or developing of new sensors.

To overcome the problem, a number of methods were investigated. One of them is using the eclipse phenomena where the satellite will always experience it in near equatorial plane (with inclination is in between 10 degree to 15 degree). The eclipse occurrence is quite frequent, as a satellite at 1000km will experience 10 eclipses per day. Eclipse can be detected from the coarse sun sensors located on each sides of the satellite (as solar panel) without needing the knowledge of satellite's attitude. As every satellite must have its own Real Time Clock (RTC) for house keeping, it can be used to measure the eclipse duration and epoch.

Three main information items can be obtained from the eclipse; time lapse between entering and leaving the shadow zone, time taken from entry (or exit) point of shadow zone to another point and time from perigee passage to entry (or exit) point of shadow zone. In this paper, this information is used to solve the orbit geometry for eclipse phenomena and then use it as input to the orbit propagator and also as innovations for the state estimation filter. Keplerian elements are used and divided into two parts: Slow

varying elements, $[a, e, i]$ and fast varying elements, $[\dot{u}, \dot{U}, \dot{\sigma}]$, where a is semi-major axis, e is eccentricity, i is inclination, u is argument of perigee, U is right ascension of ascension node and σ is true anomaly. The slow varying elements will only change slightly in one orbit and can be filtered from magnetometer data.

Knowing the slow varying elements together with eclipse epoch time (to obtain the true anomaly) the $[\dot{u}, \dot{U}]$ can be solved as eclipse phenomena will give a unique set of solution for any orbit geometry. The set contain four possible points where two of them are unlikely solutions and the most probable answer can be chosen based on entering or leaving the shadow zone. The result is used as an input to the orbit propagator and which is used in parallel to aid the solution.

Splitting the Keplerian elements into two parts give some advantages especially when magnetometer data are used to determine slow varying elements: better immunity to earth magnetic field noise when solar activity is high and better extraction of information even with small variation in magnetic field. Furthermore its small perturbation makes it possible to be smoothed using low pass filter (or average it for some period of time). Fast varying elements which have more influence in position error, will be monitored by the orbit propagator, which is running in parallel, to provide information on position of the satellite. New initial values that reset the orbit propagator are used at the instance of eclipse, based on its epoch time. Orbit information in between the eclipse can be obtained from the orbit propagator.

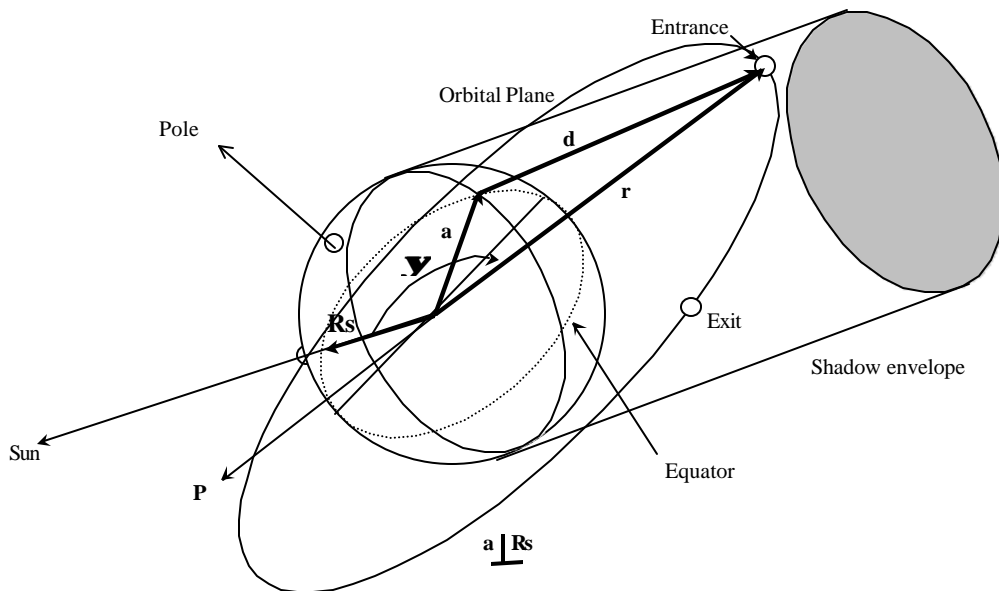


Figure 1. Orbit geometry for entry and exit point from the eclipse.

In this paper, the basic conditions and equations of eclipse are first introduced, and then the methodology of epoch time assisted orbit determination is discussed. Other variations that are investigated will be mentioned and discussed.

Eclipse Phenomena

In this section, the eclipse is analysed mathematically to build foundation for the concepts that will be discussed later. The eclipse occurs when the satellite is entering earth shadow zone. This can be done by first calculating the angle between satellite point and sun point. Assuming the shadow is in cylindrical form from round earth, the entry and exit points are located at the right angle of earth shadow line to the satellite point as in figure 1 and figure 2.

Reference [19] provide the shadow function S , which when $S = 0$ is the condition for the entry and exit point of the eclipse. The equation can also be corrected from the effect of flattening of the earth and umbra/penumbra effect of the eclipse.

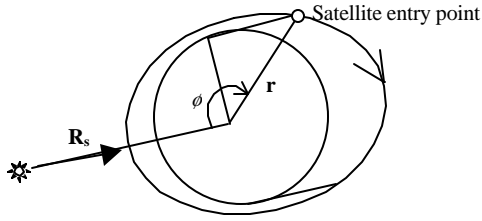


Figure 2. Eclipse from satellite orbit plane.

The angle ϕ can be obtained from the equation below

$$\cos \mathbf{y} = \frac{\mathbf{R}_s \cdot \mathbf{r}}{R_s r} \quad (1a)$$

$$\sin(180 - \mathbf{y}) = \frac{R_e}{r} \quad (1b)$$

where \mathbf{R}_s is the sun vector, \mathbf{R}_e is earth equatorial distant and \mathbf{r} is the satellite vector from the centre of the earth. The satellite vector \mathbf{r} can be represent in **PQW** frame (orbital frame) as

$$\mathbf{r} = x_w \mathbf{P} + y_w \mathbf{Q} \quad (2)$$

where it can be transform into **IJK** frame

$$\begin{aligned} x_w &= r \cos \mathbf{u} \\ y_w &= r \sin \mathbf{u} \end{aligned}$$

$$\mathbf{P} = \begin{bmatrix} \cos(\mathbf{w}) \cos(\Omega) - \sin(\mathbf{w}) \sin(\Omega) \cos(i) \\ \cos(\mathbf{w}) \sin(\Omega) + \sin(\mathbf{w}) \cos(\Omega) \cos(i) \\ \sin(\mathbf{w}) \sin(i) \end{bmatrix}$$

$$\mathbf{Q} = \begin{bmatrix} -\sin(\mathbf{w}) \cos(\Omega) - \cos(\mathbf{w}) \sin(\Omega) \cos(i) \\ -\sin(\mathbf{w}) \sin(\Omega) + \cos(\mathbf{w}) \cos(\Omega) \cos(i) \\ \cos(\mathbf{w}) \sin(i) \end{bmatrix}$$

The shadow function as has been describe in [19] and [21] as

$$S = r_e^2 (1 + e \cos v)^2 + p^2 (\mathbf{b} \cos v + \mathbf{x} \sin v)^2 - p^2 \quad (3)$$

where

$$\begin{aligned} p &= a(1 - e^2) \\ \mathbf{b} &= \frac{\mathbf{P} \cdot \mathbf{R}_s}{R_s} \\ \mathbf{x} &= \frac{\mathbf{Q} \cdot \mathbf{R}_s}{R_s} \end{aligned}$$

The time spent in earth shadow can be approximated from Keplerian motion as

$$\Delta t = \sqrt{\frac{a^3}{\mathbf{m}}} \left[\tan^{-1} \left(\frac{\sin E_2}{\cos E_2} \right) - \tan^{-1} \left(\frac{\sin E_1}{\cos E_1} \right) + e(\sin E_1 - \sin E_2) \right] \quad (4)$$

where E is the eccentric anomaly and subscript 1 and 2 indicate the entry point and exit point.

The true anomaly can be approximated from the epoch time by truncating the series expansion of Kepler's time equation as

$$\mathbf{u} = M + \left(2e - \frac{e^3}{4} \right) \sin M + \frac{5}{4} e^2 \sin 2M + \frac{13}{12} e^3 \sin 3M \quad (5)$$

Epoch Time Assisted Orbit Determination

This section will describe how the information gathered will be used in finding the orbit information. Two main strategies are investigated:

1. Instantaneous orbit determination. (Method 1): Make used the epoch time (from perigee (t_{-p}) and solve the orbit equation
2. Dynamic orbit determination. (Method 2): Make use of the epoch time for entering and leaving

the shadow zone. Two range vectors with \mathbf{D} are used to find the orbit.

In both methods, the slow varying elements must be solved first.

The slow varying elements are determined using magnetometer as in [8] but ignoring two elements $[\dot{u}, \dot{\Omega}]$.

Define the state as

$$X^T = [a, e, i, \mathbf{u}]$$

is used to estimate the slow varying element while ignoring the perturbation. The inclusion of true anomaly in the state is to produce dynamic to the filter. The true anomaly will be corrected and will be discussed later.

The Jacobian matrix, $F_k(X)$, is described by an orbit generated by a central force only based on the following state equation:

$$\dot{X} = \begin{bmatrix} 0 \\ 0 \\ 0 \\ \frac{\sqrt{\mathbf{m}}(1+e\cos\mathbf{u})^2}{\sqrt{[a(1-e^2)]^3}} \end{bmatrix}$$

where

\mathbf{m} is earth gravitational constant.

The Jacobian matrix is given by

$$F_k(X) = \frac{\partial(\dot{X})}{\partial X} = \begin{bmatrix} 0_{3 \times 4} \\ F_{4,1} & F_{4,2} & 0 & F_{4,4} \end{bmatrix}$$

where

$$F_{4,1} = \frac{1.5}{a} [\dot{X}_{4,1}]$$

$$F_{4,2} = \left[\frac{3e}{1-e^2} - \frac{2\cos\mathbf{u}}{1+e\cos\mathbf{u}} \right] [\dot{X}_{4,1}]$$

$$F_{4,4} = \frac{2e\sin\mathbf{u}}{1+e\cos\mathbf{u}} [\dot{X}_{4,1}]$$

The measurement model used is given by

$$y_k = N(\mathbf{B}(t_k)) + v_k$$

where $N(\)$ is the norm operator, \mathbf{B} is the magnetic field vector according to 2000 IGRF model based on propagated model at time k and v_k is a zero mean Gaussian white noise. An Extended Kalman Filter is constructed from this model. Reader can refer to reference [8] for more details.

The true anomaly can be found by several approaches and only some will be discussed here. Since the filter itself will provide the true anomaly, it can be used directly into the equation. From the epoch time itself, based on equation (5), true anomaly can be found explicitly. From Keplerian motion, the Mean anomaly, M , is described by

$$M = n(t - t_p)$$

where t_p is time at perigee passage. The major element affecting the anomalistic period is the J_2 effect due to oblateness of the earth, described by

$$t_a = 2\mathbf{p} \sqrt{\frac{a^3}{\mathbf{m}}} \left[1 - \frac{3J_2 r_e^2}{2a(1-e^2)} (1 - 3\sin^2 i \sin^2 \mathbf{w}) \right] \quad (6)$$

Now the perigee passage time can be described as

$$t_p = k t_a \quad (7)$$

where k is the number of successful orbit.

Once the slow varying elements have been determined, solving the non-linear equation based on the shadow equation will now solve the fast varying elements. As the shadow function, $S = 0$ at eclipse, the equation is simplified as

$$\begin{bmatrix} \cos\mathbf{u} & \sin\mathbf{u} & 0 \end{bmatrix} \begin{bmatrix} P_x & P_y & P_z \\ Q_x & Q_y & Q_z \\ W_x & W_y & W_z \end{bmatrix} \begin{bmatrix} R_{s_x} \\ R_{s_y} \\ R_{s_z} \end{bmatrix} = \frac{a_e^2 (1+e\cos\mathbf{u})^2 + p^2}{p^2} \quad (8)$$

To solve this non linear equation, one more constraining equation is needed. The position and velocity vector in orbital plane are first established as the following:

$$\bar{r}_{PQW} = \begin{bmatrix} \frac{p \cos \mathbf{u}}{1 + e \cos \mathbf{u}} \\ \frac{p \sin \mathbf{u}}{1 + e \cos \mathbf{u}} \\ 0 \end{bmatrix}$$

$$\bar{v}_{PQW} = \begin{bmatrix} \sqrt{\frac{\mathbf{m}}{p}} \sin \mathbf{u} \\ \sqrt{\frac{\mathbf{m}}{p}} (e + \cos \mathbf{u}) \\ 0 \end{bmatrix}$$

where the semi-parameter, p , also can be determined from

$$p = r(1 + e \cos v)$$

$$p = \frac{h^2}{\mathbf{m}}$$

Since the transformation matrix will not change the vector magnitude, the position and velocity vector in orbital plane can be used to construct the second equation.

$$r \sin(\mathbf{u} + \mathbf{w}) = \mathbf{i}_x \cdot \mathbf{R}_{\frac{IJK}{PQW}} \mathbf{r}_{PQW}$$

where

$$\mathbf{i}_x = [\cos \Omega \quad \sin \Omega \quad 0]^T$$

$$\mathbf{R}_{\frac{IJK}{PQW}} = \mathbf{A}_z(\mathbf{w}) \mathbf{A}_x(i) \mathbf{A}_z(\Omega)$$

and

$$\mathbf{A}_x(\bullet) = \begin{bmatrix} 1 & 0 & 0 \\ 0 & \cos(\bullet) & \sin(\bullet) \\ 0 & -\sin(\bullet) & \cos(\bullet) \end{bmatrix}$$

$$\mathbf{A}_z(\bullet) = \begin{bmatrix} \cos(\bullet) & \sin(\bullet) & 0 \\ -\sin(\bullet) & \cos(\bullet) & 0 \\ 0 & 0 & 1 \end{bmatrix}$$

Implementation of the Methods

Data from first nine months of archived SUNSAT telemetry is used for the experiment. SUNSAT is the University of Stellenbosch satellite launched in February 1999 and has ended its service in January 2002. The orbit of the satellite was 876.72 x 656.22 km with inclination of 96.4786 degree and the

satellite was experiencing eclipse for the first nine months before it was continuously in the sun for the next period. The satellite was carrying a 3-axis magnetometer, coarse and fine sun sensor, CCD type horizon sensors and GPS receiver. The satellite ephemerid obtained from NORAD Two Line Elements (TLE) archive, and it has been used to initialise the orbit propagator and compared with as a reference. Even though the satellite was carrying a high precision GPS receiver, it was operated for JPL as an experiment so there is no in flight ephemerid is available.

The suggested methods were first tested for its feasibility for the duration of available data, because very small amount of the telemetry data in the archive have all the information needed simultaneously. Simulated data is generated and used whenever the data needed is unavailable; also tested and corrected before being verified. Different types of orbit propagators are used to generate the ephemerid and SGP4 was chosen as the reference propagator.

The implementation is explained in figure 3 below where the simulation modules were tested independently for verification. The idea was tested by using the total flight time and used it to generate true anomaly. SUNSAT was maintained on weekly basis and the clock onboard was

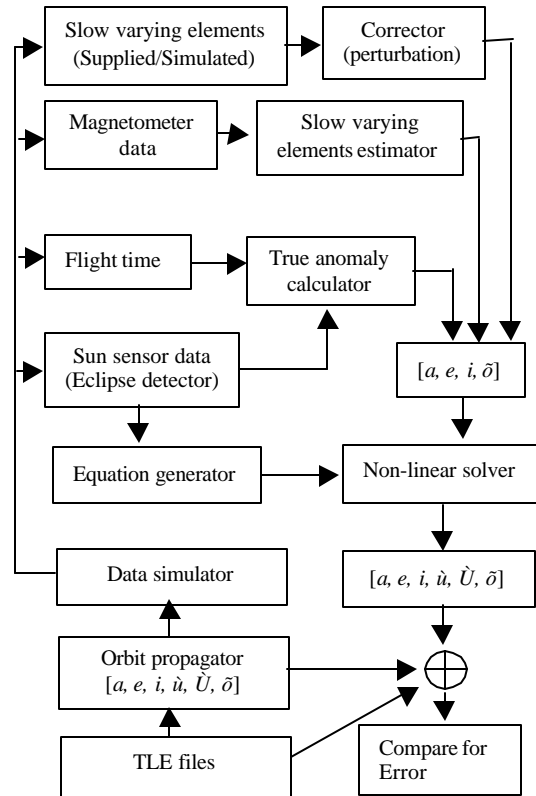


Figure 3. Simulation flowchart used to evaluate developed method.

reset during each maintenance routine. True anomaly from flight time does coincide with the true anomaly given by NORAD. At the same time, using the EKF, the slow varying elements were filtered from magnetometer data. The filter was able to track the slow varying elements $[a, e, i, \delta]$ in less than two revolutions. One of difficulties faced by this filter is to estimate $[\dot{U}, \dot{u}]$. The divergence was mainly caused by the modelling errors of these two elements.⁸ It is assumed that the filter will not diverge since the filter was not used to estimate those two elements. This could not be verified since there is no SUNSAT magnetometer data for more than 25 revolutions continuously.

A Newton based non-linear solver was used to solve the non-linear equation for $[\dot{U}, \dot{u}]$. The accuracy of $[\dot{U}, \dot{u}]$ depends on the accuracy of the sun ephemerid, tolerance set for the solver and the true anomaly. Since the $[\dot{U}, \dot{u}]$ is solved analytically, the result will converge as other Keplerian elements supplied and error tolerance is met.

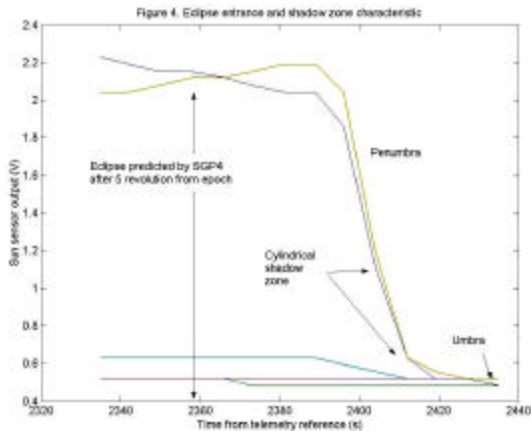


Figure 4. Eclipse entrance and shadow zone characteristic.

In predicting the eclipse, the method suggested in reference [19] was first investigated to identify the penumbra, umbra and the cylindrical shadow zone so that correct output voltage from the sun sensor can be selected as suitable threshold for the cylindrical shadow zone. Figure 4 shows the sensor output voltage for in different shadow zone and the threshold was set to be 0.75V for a cylindrical shadow. SGP4 propagator was used to generate the orbit elements but failed to predict the eclipse correctly. The accuracy of SGP4 in predicting the eclipse is in between two samples (for 8 and 10 second per sample) for the first revolution and deteriorates there after. Therefore another propagator, based on Cowell's method was then used. Since

SGP4 was used by SUNSAT for its orbit propagator onboard, it served as an orbit reference. The orbit was propagated, stored as a file and referred using its time index.

Some of the telemetry data in the archives are intermittent for certain period of the time of interest. A strategy has been established to generate a reliable source of data that can imitate the real flight data in the discontinuous segment. Simulated data were generated from orbit information propagated by SGP4 orbit propagator. The SGP4 will provide reliable orbit propagation during one revolution, before it starts to deteriorate. Therefore the SGP4 was reset at the instance of eclipse occurrence until a new epoch was reach from the TLE files. Figure 5 below show the verification of simulated data.

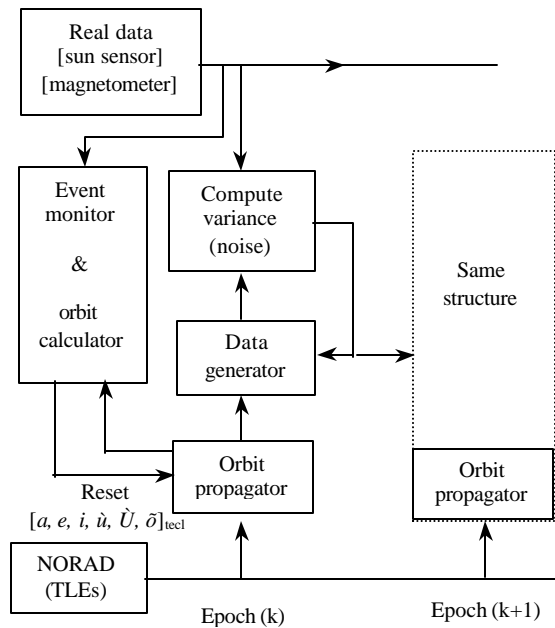


Figure 5. SUNSAT data simulator/verifier based on available knowledge of sensor data.

The variance of magnetometer noise is constantly calculated whenever data is available, by comparing the norm of calculated and measured earth magnetic field. Data was only generated whenever the sun sensor data was available to avoid the perfect occurrence of the eclipse. This also avoids required knowledge of the satellite attitude for sensor orientation.

Current and Future Works

An EKF filter was used to estimate $[a, e, i, \dot{u}, \delta]$ and used equation (8) to solve for RAAN, \dot{U} , at the instance of eclipse occurrence. The RAAN is then propagated using Variation of Parameter in order to give the full orbital elements. Using this hybrid, the position accuracy is found to be in range of 2 – 5 km, and mainly depends on

the accuracy of true anomaly. This was concluded from an experiment, where defining an artificial time to produce better true anomaly (interpolating between two samples) give greater accuracy (less than 1 km) in the first few revolutions from a known epoch. In this experiment also, the true anomaly used was from epoch time, which works fine in first few revolutions before the anomalistic time errors and on-board clock errors arise. The experiment will also be extended to propagate \dot{u} , in parallel with the filter and evaluate its accuracy compared to a known position at given epoch from existing TLE files.

At the current stage of the research, the orbit is determined analytically using the nonlinear solver: The burden of computation relies heavily on this for real time purposes. Evaluating the method is now an ongoing process with some refinements so that \dot{u} can be determined from the time in eclipse and compared to its form factor with respect to the sun line. Figure 6 below shows the graphical explanation to the determination of \dot{u} from the time in the shadow zone.

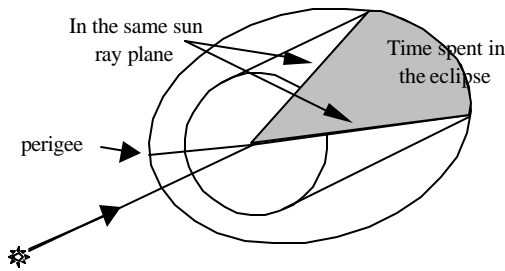


Figure 6. Time-in-eclipse to locate the perigee point.

To locate the perigee point from the sun line, can be achieved if the eccentricity of the orbit is big enough. If this can be achieved, the EKF used in the process will be forced to the corrected value at the instance of eclipse. It is planned for future work to run both orbit propagator and EKF simultaneously so that the propagated elements and estimated elements can be mixed to prevent any divergence of the filter. Both divergence and non-convergent problem in both full estimator and non-linear solver can then be avoided. This is shown in figure 6 below.

The data will be filtered to produce the estimated Keplerian elements, $[a, e, i, \dot{u}, \dot{U}, \delta]_e$, while the initial orbit will be propagated to produce analytic Keplerian elements, $[a, e, i, \dot{u}, \dot{U}, \delta]_a$. These two values will be mixed with the multipliers $[k_1, k_2]$ to weight the two. The result will be feedback to the EKF as predicted value and also used to calculate the position, velocity and acceleration vectors. Variation

of Parameters will be used to propagate the elements based on the sampling frequency. Event monitor will monitor the eclipse and calculate the new value and force the EKF to this new value. An event predictor will predict the eclipse and will correct the time of perigee passage accordingly. Note that if either $k_1 = 0$ or $k_2 = 0$, it will be in its original form, either pure propagator or estimator. The optimum value for these multipliers will be known once this method fully investigated.

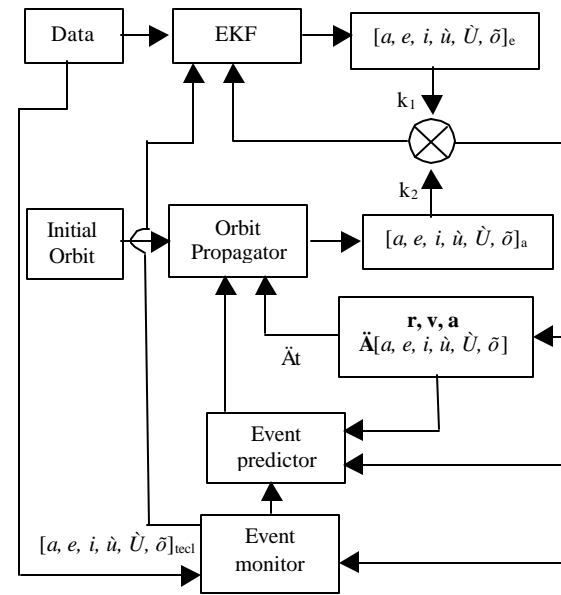


Figure 6. Hybrid orbit estimator/propagator block diagram.

Conclusion

The method of orbit determination using epoch time of the eclipse proposed is an evolution from methods that has been established but handles it with a different architecture. This work is an extension of previous investigations where the filter was used to estimate $[a, e, i, \dot{u}, \delta]$ and used the eclipse geometry to solve for \dot{U} . The method suggested could be summarised as using the slow varying elements from noisy environment by filtering the magnetometer data, while relying on the orbit geometry of the orbit at eclipse for the fast varying elements. The result is promising but inconsistencies due to convergence problems are encountered in the non-linear solver. If the non-linear solver converges, the accuracy is in between 2 – 5 km.

This is a promising method and works has been done in refining the true anomaly and finding the argument of perigee explicitly so that better accuracy can be achieve without having convergence problem in solving the orbit geometry.

References

1. Fox, S. M., Pal, P.K. and Psiaki, M., "Magnetometer-Based Autonomous Satellite Navigation (MAGNAV)." American Astronautical Society, AAS Paper 90-051: 369-382, 1990.
2. Psiaki, M, and Martel, F., "Autonomous Magnetic Navigation for Earth Orbiting Spacecraft." Third Annual AIAA/USU Conference On Small Satellites, 1989.
3. Psiaki, M., Martel, R. And Pal, P.K., "Three Axis Attitude Determination via Kalman Filtering of Magnetometer Data." Journal of Guidance, Control and Dynamics, Vol 13 (3): 506-514, 1990.
4. Psiaki, M., Huang, L. And Fox, S.M., Ground Tests of Magnetometer-Based Autonomous Navigation (MAGNAV) for Low Earth Orbiting Spacecraft, Journal of Guidance, Control and Dynamics, Vol 16 (1): 206-214, 1993
5. Psiaki, M., "Autonomous Orbit and Magnetic Field Determination Using Magnetometer and Star Sensor Data." Journal of Guidance, Control and Dynamics, Vol 18 (3): 584-592, 1995.
6. Psiaki, M., "Autonomous Low-Earth Orbit Determination from Magnetometer and Sun Sensor Data." Journal of Guidance, Control and Dynamics, Vol 22 (2): 296-304, 1999.
7. Psiaki, M., "Autonomous Orbit Determination for Two Spacecrafts from Relative Position Measurements." Journal of Guidance, Control and Dynamics, Vol 22 (2): 305-312, 1999.
8. Shorshi, G., and Bar-Itzhack, I.Y., "Satellite Autonomous Navigation Based on Magnetic Field Measurements." Journal of Guidance, Control and Dynamics, Vol 18 (4): 843-850. 1995.
9. Wiegand, M., "Autonomous Satellite Navigation via Kalman Filtering of Magnetometer Data." Acta Astronautica, Vol. 38 (4-8): 395-403, 1996.
10. Hicks, K.D. and Wiesel, W.E., Autonomous Orbit Determination Systems for Earth Satellite. Journal of Guidance, Control and Dynamics, Vol 15 (3): 562-567, 1992.
11. Nagarajan, N., Bhat, M.S. and Kasturirangan, "A Novel Autonomous Orbit Determination System Using Earth Sensor (Scanner)." Acta Astronautica, Vol. 25 (2): 77-84, 1991.
12. Sanusi, H. and du Plessis, J.J. Investigations of Using Epoch Time in Correction of Geomagnetic Models, In Estimating The Orbit For Low Earth Equatorial Orbit Satellites. 2nd International Conference on Advances in Strategic Technologies, Malaysia, Oct. 2000.
13. Chory, M., Hoffman, D.P. and LeMay, J.L., "Satellite Autonomous Navigation – Status and History." *Proceeding of IEEE Position, Location and Navigation Symposium* (Las Vegas, NV), Institute of Electric and Electronic Engineer, New York: 110-121, 1986.
14. Raol, J.R. and Sinha, N.K., "On the Orbit Determination Problem." *IEEE Transaction on Aerospace and Electronic Systems*, Vol AES-21 (3): 274-290, 1985.
15. Tai, F. And Noerdlinger, P.D., "A Low Cost Autonomous Navigation System." *American Astronautical Society*, AAS Paper 89-001: 3-23, 1989.
16. Hosken, R. And Wertz, J.R., "Microcosm Autonomous Navigation System On-Orbit Operation." *American Astronautical Society*, AAS Paper 95-074: 491-506, 1995.
17. Konigsmann, H.J., Collins, J. T., Dawson, S. And Wertz, J. R., "Autonomous Orbit Maintenance System." *Acta Astronautica*, Vol. 9 (9-12): 977-985, 1996.
18. Bate, R.R., Mueller D.D. and White, J.E., "Fundamentals Of Astrodymanics." Dover Pub. Inc, New York , 1971.
19. Escobal, P.R., "Methods of Orbit Determinations." John Wiley & Sons, Inc, New York , 1965.
20. Sidi, M., "Spacecraft Dynamics and Controls." Cambridge University Press, New York , 1997.
21. Vallado, D. A., "Fundamentals of Astrodynamics and Applications." McGraw-Hill, New York, 1997.
22. Wertz, J.R. (Ed.), "Spacecraft Attitude Determination and Control." Kluwer Academic Pub, Dordrecht, 1978.
23. Jordaán, J.J., "An Extended Kalman Filter Observer for Autonomous Orbit Determination." Master's thesis: University of Stellenbosch, 1996.
24. du Plessis, J. A. F., "Low Earth Orbit Satellite Propagators." Master's thesis: University of Stellenbosch, 1999.